NASA-CR-193280

IN-43-CR
175329

Final Report: NASW-4700 Occultation of Neptune Radio Emission at a Magnetic Ridge

Neptune High-Latitude Emission: Dependence of Angle on Frequency

p- 11

ABSTRACT

Smooth broadband radio emission reached a maximum and then cut off as Voyager approached the north magnetic pole of Neptune. The time of each event depends on frequency, yielding information on radio source location and emission angle. In a preliminary analysis L-shell and magnetic longitude define radio- source locations in a dipole field. The emission angle at each frequency is identified with the angle between the magnetic-field direction at the source and the line of sight to Voyager 2 at the time of emission maximum. At each value of L in the range $6 < L < 9$, there is one source longitude for which emission angle varies smoothly from $\geq 90^{o}$ at 40 kHz to as low as 20^{o} at 462 kHz. A more complex magnetic-field model can give a qualitatively different result.

INTRODUCTION

At Neptune the Planetary Radio Astronomy (PRA) experiment observed radio emission, presumably at the electron cyclotron frequency, in the range 20 to 1326 kHz corresponding to magnetic field of 714 to 47,357 nT. The magnetometer on Voyager measured fields as strong as 9,695 nT (271 kHz). Voyager must have passed through source surfaces corresponding to frequencies lower than 271 kHz. The associated radio event (except possibly at 39.6 kHz) is not a simple occultation at time of passage. At frequencies as high as 462 kHz a drop in intensity accompanies a change in sense of circular polarization. *Sawyer et al.* [1992] suggested that a remote source is occulted by an intervening ridge in the constant-frequency surface.

We proposed and contracted to determine emission angles and describe the occulter in the framework of the offset tilted dipole (OTD2) model of the magnetic field. A few months after the proposal *Connerney et al.* [1991] published the spherical harmonic magnetic model, which is more complex than a dipole, describing multiple poles and dip equators. The model represents the magnetometer measurements along the spacecraft trajectory. The field at remote radio sources is known less precisely. The magnetic modelers recommend including terms of order and degree three to represent the field at off-trajectory locations. We examined the characteristics of the field described by the O8 model and found it to be very different from the OTD2 model in the region where radio sources are located. An interim report on these conclusions was submitted to the NDAP program in January 1993, addressed to Jay Bergstrahl.

This final report describes a study that uses the second-order OTD2 model (Ness 1989) to develop a method of analysis of the frequency dependence of the times of maximum emission and of emission cutoff. Assuming that sources are on one field line we found at each value of L a source longitude that gives a smooth progression of emission angle with frequency. At the high-latitude location the direction of the OTD2 field is largely radial. The O8 field at the same location is, however, nearly meridional, so that emission angles from sources at that location would be approximately complimentary to those determined by the OTD2 analysis. Sources at different frequencies would then lie on different field lines, at the top of loops . The concept that sources of different frequency lie on a single field line requires that the field line have a significant radial

component, as in the vicinity of a magnetic pole. This concept underlies the method of analysis described here. The procedure could produce useful information, but specific results based on the OTD2 model are probably misleading.

OBSERVATIONS

The times of emission maxima and of cutoffs measured at 12 frequencies from 39.6 to 462 kHz are shown in Table 1 and Table 2. Events occur later at higher frequency, but not in smooth progression. The cutoff of emission from the f = 39.6 kHz source occurs close to the time when the measured magnetic field at Voyager corresponds to electron cyclotron frequency f_c = 39.6 kHz. At this time the line of sight from source to Voyager must lie almost parallel to the constant-frequency source surface. At higher frequencies cutoff occurs when the local measured f_c at Voyager is considerably less than the observed cutoff frequency f, that is, when Voyager is well above the corresponding source surface. The line of sight at emission maximum and at cutoff of the higher frequencies must have a relatively large radial component, except at the lowest frequency. This conclusion is drawn from the magnetometer measurements and is independent of any magnetic model.

The cutoff at each frequency is accompanied by a left-to-right reversal of apparent circular polarization. *Sawyer et al.* [1989, 1992] interpreted this as occultation of extraordinary-mode (X-mode) emission, leaving weaker ordinary-mode (O-mode) emission. In the outward directed dipole field in the northern hemisphere, the apparent left-hand circular polarization must be "False" if it is X-mode, that is, the source direction must lie on the side of the antenna electric plane where the instrument records polarization of opposite sense to that of the incident wave. Figure 6a of *Ladreiter et al.* [1991] shows the radio horizon, enclosing the region on the 39.6 kHz surface from which X mode can propagate to Voyager at the time of emission maximum. This is based on the OTD2 magnetic model. Figure 1 shows that the situation is actually more complex, even in the OTD2 framework. The antenna electric plane cuts through the visible portion of the radio surface enclosed by the radio horizon. Apparent polarization is "True" in the larger, northeastern part, and "False" only in the southwestern part. In the outward-directed OTD2 field left-hand X-mode emission can come from the smaller "False" area.

MODELED MAGNETIC FIELD

Figure 2 shows the non-radial component of the magnetic field described by the spherical-harmonic O8 model. It is plotted on the 154.8-kHz constant-frequency surface. At magnetic poles the radial field appears on this plot as a very small vector or a dot. A downward-directed magnetic pole near latitude 45°, longitude 120° dominates the region visible from Voyager at the time of the emission maxima and cutoffs. At latitude 60°, longitude 128°, the source location found on the basis of the OTD2 model, the field is mainly non-radial. It is approximately normal to the direction of the OTD2 model field at this location. (Of course, there is no reason to believe that the solution in the O8 model would give the same location as in the OTD2 model.) The region

of converging arrows marks downward-directed field. In this region, outward-directed X-mode emission would be left-hand circularly polarized. The PRA would measure this emission as left-hand polarized if the source lay on the "True" side of the electric plane. When the radio horizon and electric plane are projected on the constant-frequency surface described by the O8 model, the picture is more complex, with several separate domains of apparent polarization sense in the visible region.

ANALYSIS

Emission Angle: The analysis is based on the OTD2 magnetic model. This is useful for developing the method and for comparison with earlier studies. Because of strong dependenceon the magnetic model, specific results are not expected to be realistic. The time of maximum emission (or cutoff) defines the location and attitude of Voyager. The value of L, with the frequency, determines the latitude and radial position component of the source in the dipole field. At each L, calculations were made for different assumptions concerning source longitude. For each assumed source position the necessary values were computed and printed in Table 1 and Table 2:

Spacecraft event time, SCET, is the time of maximum or cutoff at the given frequency.

Source radial distance from the dipole center (rm) and latitude (slat) are found from the frequency and L value. The angle between the radius and the field direction is labeled anglrB.

Voyager dipole distance (rvd), latitude (vlat), and longitude (vlon) are found from the Voyager ephemeris.

The Cartesian components in dipole coordinates of the vector from dipole center to source (xsd), dipole center to Voyager (xvd), and source to Voyager (xvs) are listed.

The emission angle, labeled "a bsv", is the angle between the source-Voyager vector xvs and the field direction. The angle b between the magnetic field **B** and the ray **k** is found by equating cos b to the normalized dot product of **B** and the vector **SV**.

Rmin is the minimum distance from the planet center of the line of sight. A value less than 1 implies occultation of the source by the planet as seen from Voyager.

In the time interval between the earliest low-frequency emission maximum at 0313 SCET and the latest high-frequency cutoff at 0340 the dipole distance of Voyager decreased from almost $3R_N$ to less than $2R_N$. Voyager's magnetic longitude changed from 90° to 156°, and its latitude from 63° to 73°. Values of emission angle are plotted against the logarithm of the frequency for different source longitudes at a given L value in Figure 3. An approximate balance among the three changing components of source-spacecraft distance, especially the radial and longitudinal components, makes it possible to find a source longitude at each L value that gives a smooth variation of emission angle with frequency, even though the maximum times and cutoff times do not themselves vary smoothly or even in sequence.

All of the curves representing sources distributed over an extended longitude range show large oscillations and irregularities. When sources are distributed in longitude, the source nearest

Voyager dominates This effectively eliminates the variation of longitude difference that is needed to balance the changing radial component of the distance. When there is no balancing longitudinal component, the radial component by itself shows all the irregularity of the time sequence.

The source longitude that gives a smooth variation of emission angle varies from 125° at L = 10 to 165° at L = 4.5. At small L values the emission angle becomes considerably larger than 90°. This would predict that the polarization sense changes with frequency, which is not observed with this event. Also at small L, the value of R_{min} is much less than 1 for high frequencies. In the OTD2 model the dipole offset fits the distant field. This leads to greater asymmetry of high-frequency source surfaces than in a model that includes higher-order terms. The small distance (rmin) from planet center to the 462 kHz source is the result of the field model.

The data indicate a preferred solution with L = 8.6, longitude 128°. For a dipole-like field, electron precipitation is expected east of the minimum B longitude, that is, at west longitudes smaller than 150° [*Cheng* 1990].

Occulter: The work statement includes location of the occulter, as well as of the radio source. Because sources and spacecraft are close together, a ridgelike occulter lying between them has a well defined location. The O8 model suggests that the topographic feature associated with occultation might better be described as a depression. Elevation (distance from planet center) of a constant-frequency surface defined by the O8 model varies by more than a factor of two. The surface is elevated near poles, and depressed in regions of weak field where the direction of the field reverses. There is a generally low region in the northern hemisphere in an extended range of longitude around 90°. Rather than the occulting ridge envisaged by *Sawyer et al.* [1992], the topography of the O8 model suggests that Voyager views a large depression, with radio sources located on the near slope. The cartoon constructed to illustrate the effect of an intervening ridge, Figure 3 of *Sawyer et al.* [1992], applies equally well to a depressed source location. It illustrates cutoff at successively higher frequencies as the spacecraft, moving toward the north magnetic pole and in the direction of increasing magnetic west longitude, approaches the planet.

DISCUSSION

The ordering of times of peak emission determines a unique source longitude at each L value. The OTD2 magnetic model is so different from the more complex spherical harmonic model at the source site that the solution cannot be physically meaningful. Field direction changes rapidly with distance in the vicinity of the quadrupole. The range of field direction at the sources of different frequency must be greater than in a dipole model. Field-direction variation might explain some of the variation attributed in the OTD2 analysis to a broad range of emission angle. If the sources are near the quadrupole -- in its auroral region, so to speak -- the field is again nearly radial and sources of different frequency can reside on the same field line.

A question that arises in considering radio sources at the quadrupole is how the magnetically closed region can be supplied with energetic electrons.

Extension of the method of analysis to the more complex spherical harmonic model would require:
Numerical solution for the constant-frequency surface.
Numerical tracing of a field line, instead of the analytic L shell.

RECOMMENDATIONS

1. It is important to recognize that a dipole magnetic model fails to describe the magnetic environment of Neptune radio sources. Results of analysis of radio data depend on the magnetic model in a fundamental way.

2. It is important to recognize that the response of the PRA antennas to radio emission cannot be usefully described by a radio-source location at planet center.

3. Instrument response depends on the characteristics of the incident wave. Response must be calculated for each situation.

4. We should try to take into account the effects of polarization transfer between source and antennas -- the "limiting polarization region" for a radio wave.

REFERENCES

Cheng, A.F., Global magnetic anomaly and aurora of Neptune, *Geophys. Res. Lett., 17*, 1697-1700, 1990.

Connerney, J.E.P., M. Acuna, and N. Ness, The magnetic field of Neptune, *J. Geophys. Res., 96*, 19,023-19,042, 1991.

Ladreiter, H.P., Y. Leblanc, G.K.F. Rabl, and H.O. Rucker, Emission characteristics and source location of the smooth Neptunian kilometric radiation, *J. Geophys. Res., 96*, 19,101-19,110, 1991.

Ness, N.F. *private communication*, 1990.

Sawyer, C.B., K.L. Neal, and J.W. Warwick, Polarization model applied to Uranian radio emission, *J. Geophys. Res., 96*, 5575-5590, 1991.

Sawyer, C., J.W. Warwick, and J.H. Romig, Smooth radio emission and a new emission at Neptune, *Geophys. Res. Let., 17*, 1645-1648, 1990.

Sawyer, C., J.W. Warwick, and J.H. Romig, The effect of magnetic topography on high-latitude radio emission at Neptune, *J. Geophys. Res., 97*, 1-9, 1992.

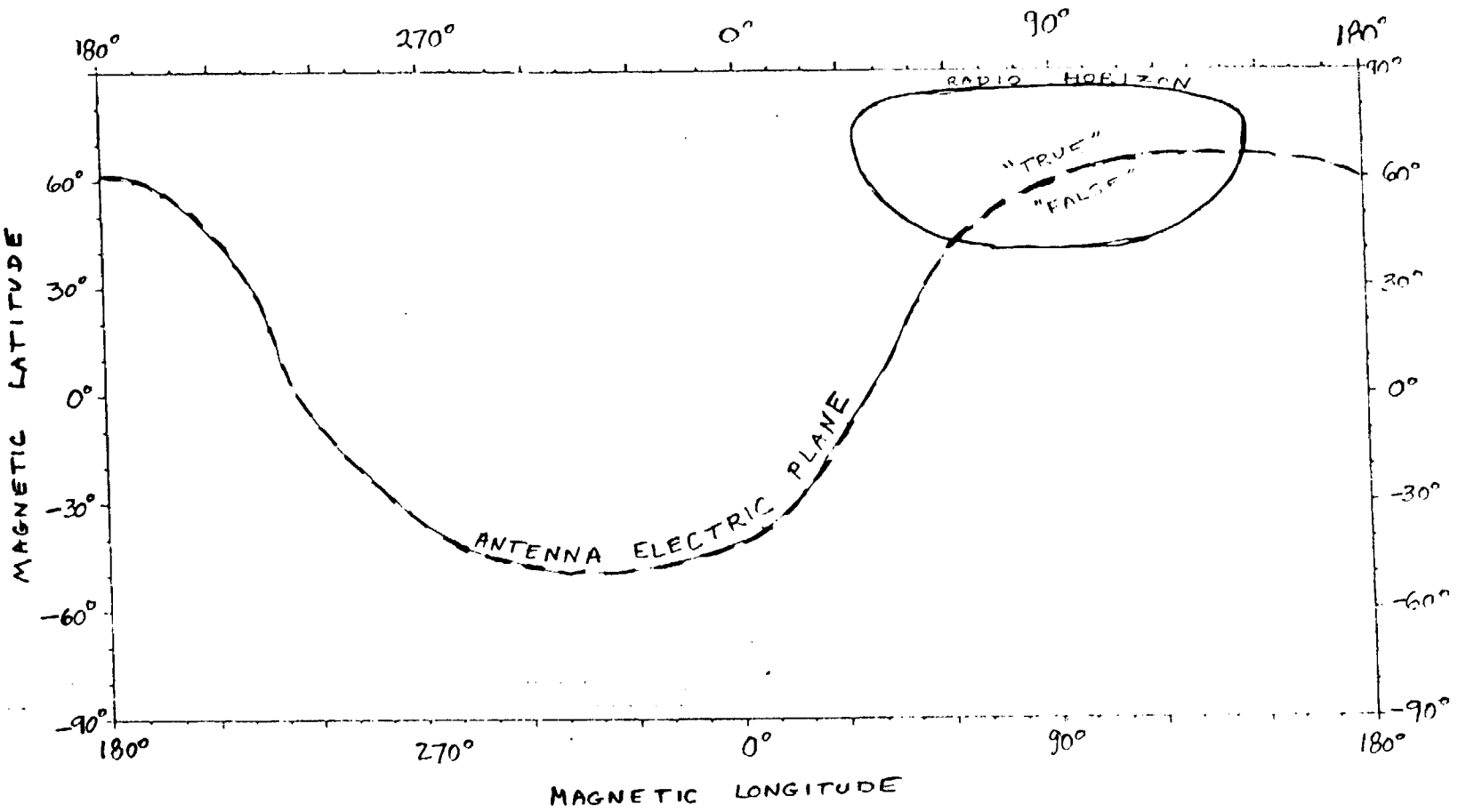

Fig. 1. Magnetic laitude and magnetic west longitude are the coordinates on the 39.6-kHz constant-frequency surface of the OTD2 offset tilted dipole magnetic-field model. The closed curve is the radio horizon, surrounding the small area on the surface from which extraordinary-mode emission could propagate to Voyager 2 as the spacecraft approaches the surface. The dashed curve is the projection on the surface of the electric plane of the PRA antennas. The apparent sense of circular polarization recorded by the PRA instrument reverses at the electric plane. The side of the plane on which the recorded polarization is opposite to that of the incident wave is labeled "False". At the time of maximum emission at 39.6 kHz, some visible source locations were in the "False" region, and others in the "True" region, according to analysis based on the OTD2 model. A more complex and presumably more realistic magnetic model has anomalous poles and dip equators, resulting in islands of opposite polarity in each hemisphere. Moreover, topographical irregularity of the constant-frequency surface in the more complex model produces an asymmetrical and convoluted radio horizon.

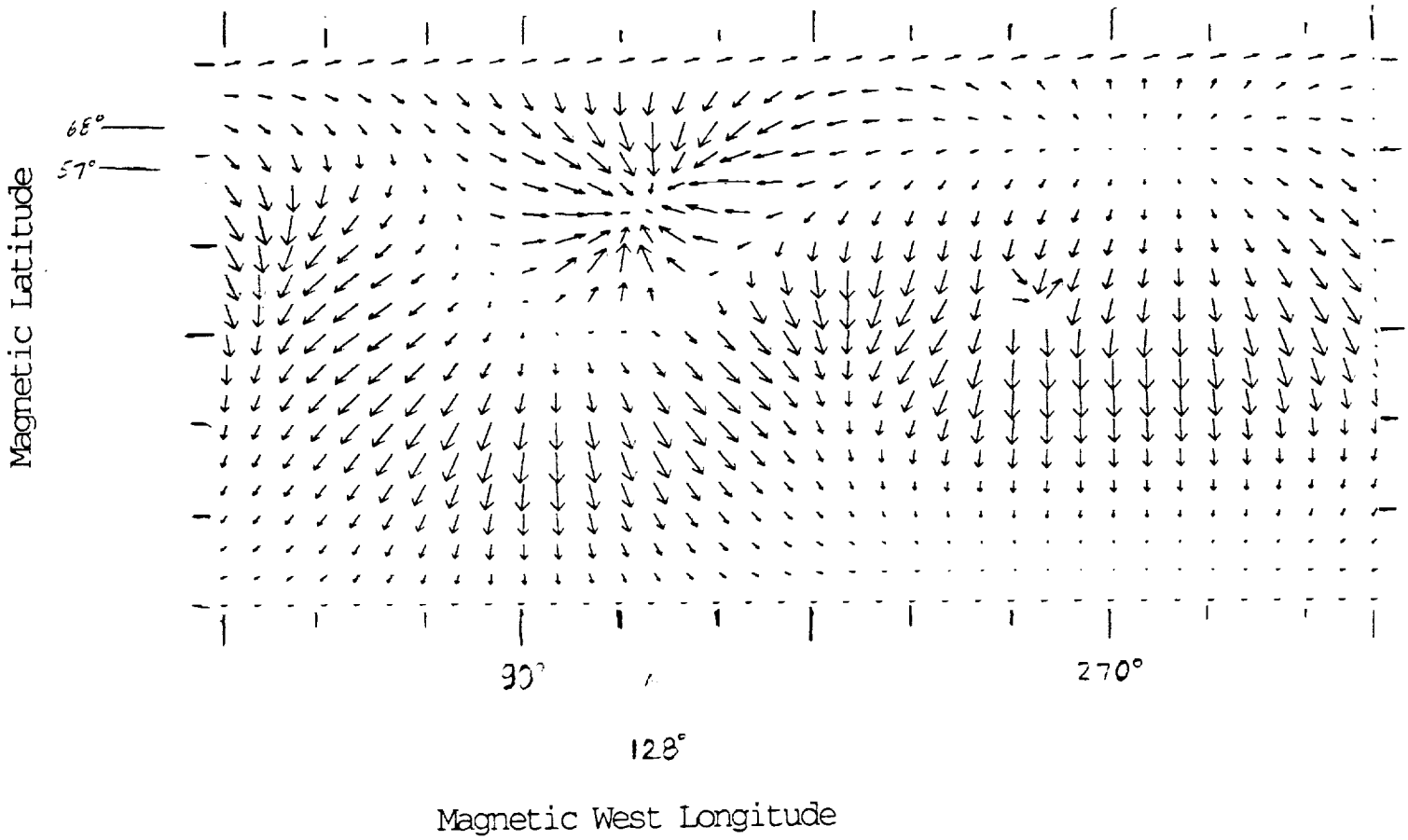

Fig. 2. The non-radial component of the O8 magnetic model is plotted on the 154.8-kHz constant-frequency surface. O8 is a spherical harmonic model of degree and order 3 with 15 coefficients. Arrows at longitude 128o and latitude 57 to 68o show the location *in the OTD2 model field* of proposed radio sources that fit the frequency dependence of the time of maximum emission. This location corresponds to reversed magnetic polarity and non-radial field direction.

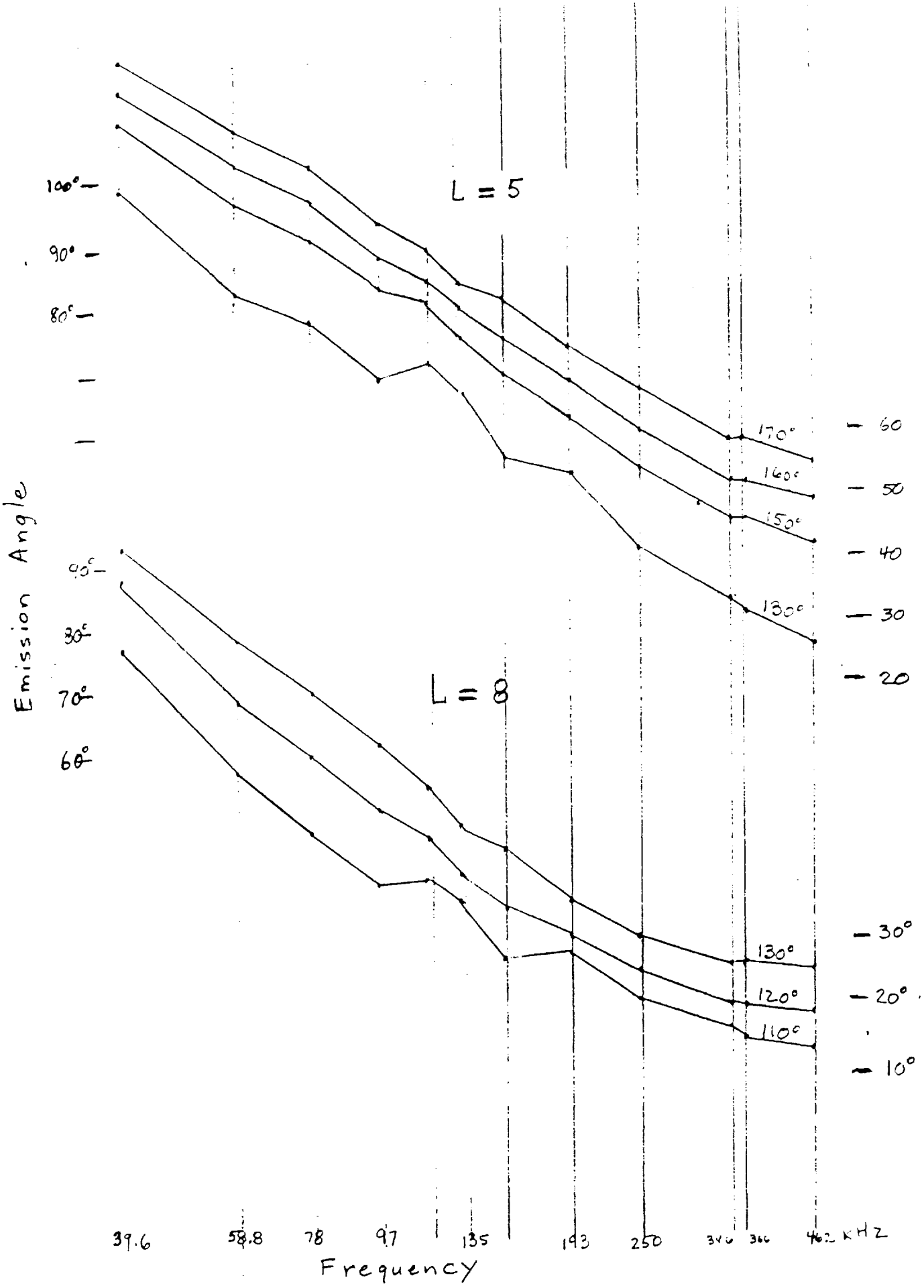

Fig. 3. The emission angle is the angle between the direction of the magnetic field at the radio source and the line of sight from source to Voyager at the time of maximum emission. At each value of magnetic L shell in the OTD2 field there is one source longitude for which the value of emission angle varies smoothly with frequency.

Table 1: **Maximum** time and emission angle at each frequency for different L shells (OTD2)

MagModl: 0.133 45.20 13.50 0.190 0.485-0.191 165.0 :source mag long; 4.5 :L

Freq	SCET	rm	anglrB	rvd	slat	vlat	vlon	xsd			xvd			xvs		a bsv	Rmin
39.6	13.3	2.44	28.5	2.97	42.6	57.3	90.2	-1.7	-0.5	1.7	0.0	-1.6	2.5	1.7	-1.1	0.9	120.2	1.84
58.8	13.4	2.16	25.7	2.97	46.1	57.4	90.3	-1.4	-0.4	1.6	0.0	-1.6	2.5	1.4	-1.2	0.9	108.9	1.61
78.0	21.2	1.98	23.9	2.65	48.4	62.3	99.9	-1.3	-0.3	1.5	-0.2	-1.2	2.3	1.1	-0.9	0.9	103.1	1.44
97.2	21.1	1.85	22.7	2.66	50.1	62.2	99.8	-1.1	-0.3	1.4	-0.2	-1.2	2.3	0.9	-0.9	0.9	96.1	1.31
116.4	29.1	1.75	21.8	2.35	51.4	67.8	115.3	-1.1	-0.3	1.4	-0.4	-0.8	2.2	0.7	-0.5	0.8	92.5	1.21
135.6	30.0	1.67	21.0	2.32	52.5	68.4	117.6	-1.0	-0.3	1.3	-0.4	-0.8	2.2	0.6	-0.5	0.8	87.1	1.13
154.8	27.1	1.60	20.4	2.43	53.4	66.4	110.5	-0.9	-0.2	1.3	-0.3	-0.9	2.2	0.6	-0.7	0.9	81.9	1.06
193.2	31.0	1.49	19.4	2.28	54.8	69.1	120.5	-0.8	-0.2	1.2	-0.4	-0.7	2.1	0.4	-0.5	0.9	74.4	0.95
250.8	29.8	1.38	18.4	2.33	56.4	68.3	117.1	-0.7	-0.2	1.1	-0.4	-0.8	2.2	0.3	-0.6	1.0	66.7	0.83
346.8	29.8	1.24	17.1	2.33	58.3	68.3	117.1	-0.6	-0.2	1.1	-0.4	-0.8	2.2	0.2	-0.6	1.1	58.3	0.70
366.0	28.4	1.22	17.0	2.38	58.6	67.3	113.5	-0.6	-0.2	1.0	-0.4	-0.8	2.2	0.2	-0.7	1.2	58.1	0.68
462.0	27.1	1.13	16.2	2.43	59.9	66.4	110.5	-0.5	-0.1	1.0	-0.3	-0.9	2.2	0.2	-0.8	1.2	54.4	0.60

MagModl: 0.133 45.20 13.50 0.190 0.485-0.191 160.0 :source mag long; 5.0 :L

Freq	SCET	rm	anglrB	rvd	slat	vlat	vlon	xsd			xvd			xvs		a bsv	Rmin
39.6	13.3	2 46	26.2	2.97	45.4	57.3	90.2	-1.6	-0.6	1.8	0.0	-1.6	2.5	1.6	-1.0	0.7	114.9	1.88
58.8	13.4	2.18	23.7	2.97	48.7	57.4	90.3	-1.4	-0.5	1.6	0.0	-1.6	2.5	1.3	-1.1	0.9	103.1	1.63
78.0	21.2	2.00	22.2	2.65	50.8	62.3	99.9	-1.2	-0.4	1.5	-0.2	-1.2	2.3	1.0	-0.8	0.8	97.3	1.45
97.2	21.1	1.87	21.1	2.66	52.3	62.2	99.8	-1.1	-0.4	1.5	-0.2	-1.2	2.3	0.9	-0.8	0.9	89.9	1.32
116.4	29.1	1.76	20.3	2.35	53.6	67.8	115.3	-1.0	-0.4	1.4	-0.4	-0.8	2.2	0.6	-0.4	0.8	86.3	1.21
135.6	30.0	1.68	19.6	2.32	54.6	68.4	117.6	-0.9	-0.3	1.4	-0.4	-0.8	2.2	0.5	-0.4	0.8	80.6	1.13
154.8	27.1	1.61	19.0	2.43	55.4	66.4	110.5	-0.9	-0.3	1.3	-0.3	-0.9	2.2	0.5	-0.6	0.9	75.3	1.06
193.2	31.0	1.50	18.1	2.28	56.8	69.1	120.5	-0.8	-0.3	1.3	-0.4	-0.7	2.1	0.4	-0.4	0.9	67.7	0.95
250.8	29.8	1.38	17.2	2.33	58.3	68.3	117.1	-0.7	-0.2	1.2	-0.4	-0.8	2.2	0.3	-0.5	1.0	60.0	0.84
346.8	29.8	1.25	16.1	2.33	60.0	68.3	117.1	-0.6	-0.2	1.1	-0.4	-0.8	2.2	0.2	-0.6	1.1	52.0	0.70
366.0	28.4	1.23	15.9	2.38	60.3	67.3	113.5	-0.6	-0.2	1.1	-0.4	-0.8	2.2	0.2	-0.6	1.1	51.9	0.68
462.0	27.1	1.14	15.2	2.43	61.5	66.4	110.5	-0.5	-0.2	1.0	-0.3	-0.9	2.2	0.2	-0.7	1.2	48.6	0.60

MagModl: 0.133 45.20 13.50 0.190 0.485-0.191 150.0 :source mag long; 6.0 :L

Freq	SCET	rm	anglrB	rvd	slat	vlat	vlon	xsd			xvd			xvs		a bsv	Rmin
39.6	13.3	2.50	22.9	2.97	49.8	57.3	90.2	-1.4	-0.8	1.9	0.0	-1.6	2.5	1.4	-0.8	0.6	105.2	1.94
58.8	13.4	2.21	20.9	2.97	52.6	57.4	90.3	-1.2	-0.7	1.8	0.0	-1.6	2.5	1.2	-0.9	0.7	92.1	1.65
78.0	21.2	2.02	19.6	2.65	54.5	62.3	99.9	-1.0	-0.6	1.6	-0.2	-1.2	2.3	0.8	-0.6	0.7	85.9	1.47
97.2	21.1	1.89	18.7	2.66	55.9	62.2	99.8	-0.9	-0.5	1.6	-0.2	-1.2	2.3	0.7	-0.7	0.8	77.9	1.33
116.4	29.1	1.78	18.0	2.35	57.0	67.8	115.3	-0.8	-0.5	1.5	-0.4	-0.8	2.2	0.5	-0.3	0.7	73.9	1.23
135.6	30.0	1.70	17.4	2.32	57.9	68.4	117.6	-0.8	-0.5	1.4	-0.4	-0.8	2.2	0.4	-0.3	0.7	67.8	1.15
154.8	27.1	1.63	17.0	2.43	58.6	66.4	110.5	-0.7	-0.4	1.4	-0.3	-0.9	2.2	0.4	-0.5	0.8	62.4	1.08
193.2	31.0	1.51	16.2	2.28	59.8	69.1	120.5	-0.7	-0.4	1.3	-0.4	-0.7	2.1	0.2	-0.3	0.8	54.7	0.97
250.8	29.8	1.39	15.4	2.33	61.2	68.3	117.1	-0.6	-0.3	1.2	-0.4	-0.8	2.2	0.2	-0.4	0.9	47.5	0.85
346.8	29.8	1.25	14.4	2.33	62.8	68.3	117.1	-0.5	-0.3	1.1	-0.4	-0.8	2.2	0.1	-0.5	1.0	40.3	0.72
366.0	28.4	1.23	14.3	2.38	63.1	67.3	113.5	-0.5	-0.3	1.1	-0.4	-0.8	2.2	0.1	-0.6	1.1	40.4	0.70
462.0	27.1	1.14	13.6	2.43	64.1	66.4	110.5	-0.4	-0.2	1.0	-0.3	-0.9	2.2	0.1	-0.7	1.2	37.8	0.61

MagModl: 0.133 45.20 13.50 0.190 0.485-0.191 135.0 :source mag long; 7.0 :L

Freq	SCET	rm	anglrB	rvd	slat	vlat	vlon	xsd			xvd			xvs		a bsv	Rmin
39.6	13.3	2.52	20.6	2.97	53.1	57.3	90.2	-1.1	-1.1	2.0	0.0	-1.6	2.5	1.1	-0.5	0.5	92.5	1.98
58.8	13.4	2.23	18.9	2.97	55.7	57.4	90.3	-0.9	-0.9	1.8	0.0	-1.6	2.5	0.9	-0.7	0.7	76.7	1.68
78.0	21.2	2.04	17.8	2.65	57.4	62.3	99.9	-0.8	-0.8	1.7	-0.2	-1.2	2.3	0.6	-0.4	0.6	69.5	1.49
97.2	21.1	1.90	17.0	2.66	58.6	62.2	99.8	-0.7	-0.7	1.6	-0.2	-1.2	2.3	0.5	-0.5	0.7	60.6	1.36
116.4	29.1	1.79	16.3	2.35	59.6	67.8	115.3	-0.6	-0.6	1.5	-0.4	-0.8	2.2	0.3	-0.2	0.6	57.1	1.25
135.6	30.0	1.71	15.8	2.32	60.4	68.4	117.6	-0.6	-0.6	1.5	-0.4	-0.8	2.2	0.2	-0.2	0.7	51.1	1.17
154.8	27.1	1.63	15.4	2.43	61.1	66.4	110.5	-0.6	-0.6	1.4	-0.3	-0.9	2.2	0.2	-0.4	0.8	44.9	1.10
193.2	31.0	1.52	14.8	2.28	62.2	69.1	120.5	-0.5	-0.5	1.3	-0.4	-0.7	2.1	0.1	-0.2	0.8	39.2	0.99
250.8	29.8	1.40	14.0	2.33	63.4	68.3	117.1	-0.4	-0.4	1.3	-0.4	-0.8	2.2	0.1	-0.3	0.9	32.4	0.87
346.8	29.8	1.26	13.2	2.33	64.9	68.3	117.1	-0.4	-0.4	1.1	-0.4	-0.8	2.2	0.0	-0.4	1.0	26.5	0.74
366.0	28.4	1.24	13.0	2.38	65.1	67.3	113.5	-0.4	-0.4	1.1	-0.4	-0.8	2.2	0.0	-0.5	1.1	26.3	0.72
462.0	27.1	1.15	12.5	2.43	66.1	66.4	110.5	-0.3	-0.3	1.0	-0.3	-0.9	2.2	0.0	-0.6	1.2	24.3	0.63

MagModl: 0.133 45.20 13.50 0.190 0.485-0.191 130.0 :source mag long; 8.0 :L

Freq	SCET	rm	anglrB	rvd	slat	vlat	vlon	xsd			xvd			xvs		a bsv	Rmin
39.6	13.3	2.54	18.8	2.97	55.7	57.3	90.2	-0.9	-1.1	2.1	0.0	-1.6	2.5	0.9	-0.5	0.4	85.8	2.00
58.8	13.4	2.24	17.3	2.97	58.0	57.4	90.3	-0.8	-0.9	1.9	0.0	-1.6	2.5	0.8	-0.7	0.6	69.0	1.71
78.0	21.2	2.05	16.3	2.65	59.6	62.3	99.9	-0.7	-0.8	1.8	-0.2	-1.2	2.3	0.5	-0.4	0.6	60.2	1.51
97.2	21.1	1.91	15.6	2.66	60.8	62.2	99.8	-0.6	-0.7	1.7	-0.2	-1.2	2.3	0.4	-0.5	0.7	51.5	1.38
116.4	29.1	1.80	15.1	2.35	61.7	67.8	115.3	-0.5	-0.7	1.6	-0.4	-0.8	2.2	0.2	-0.1	0.6	46.8	1.27
135.6	30.0	1.71	14.6	2.32	62.4	68.4	117.6	-0.5	-0.6	1.5	-0.4	-0.8	2.2	0.1	-0.1	0.6	41.3	1.19
154.8	27.1	1.64	14.3	2.43	63.1	66.4	110.5	-0.5	-0.6	1.5	-0.3	-0.9	2.2	0.1	-0.3	0.8	35.7	1.12
193.2	31.0	1.53	13.7	2.28	64.1	69.1	120.5	-0.4	-0.5	1.4	-0.4	-0.7	2.1	0.0	-0.2	0.8	30.9	1.01
250.8	29.8	1.40	13.0	2.33	65.2	68.3	117.1	-0.4	-0.5	1.3	-0.4	-0.8	2.2	0.0	-0.3	0.9	24.8	0.89
346.8	29.8	1.26	12.2	2.33	66.6	68.3	117.1	-0.3	-0.4	1.2	-0.4	-0.8	2.2	-0.1	-0.4	1.0	19.8	0.75
366.0	28.4	1.24	12.1	2.38	66.8	67.3	113.5	-0.3	-0.4	1.1	-0.4	-0.8	2.2	-0.1	-0.5	1.1	19.7	0.73
462.0	27.1	1.15	11.6	2.43	67.7	66.4	110.5	-0.3	-0.3	1.1	-0.3	-0.9	2.2	-0.1	-0.6	1.2	18.3	0.65

MagModl: 0.133 45.20 13.50 0.190 0.485-0.191 128.0 :source mag long; 8.6 :L

Freq	SCET	rm	anglrB	rvd	slat	vlat	vlon	xsd			xvd			xvs		a bsv	Rmin
39.6	13.3	2.55	18.0	2.97	57.0	57.3	90.2	-0.9	-1.1	2.1	0.0	-1.6	2.5	0.8	-0.5	0.4	82.7	2.02
58.8	13.4	2.25	16.6	2.97	59.3	57.4	90.3	-0.7	-0.9	1.9	0.0	-1.6	2.5	0.7	-0.7	0.6	65.5	1.72
78.0	21.2	2.05	15.6	2.65	60.8	62.3	99.9	-0.6	-0.8	1.8	-0.2	-1.2	2.3	0.4	-0.4	0.6	55.8	1.52
97.2	21.1	1.91	15.0	2.66	61.9	62.2	99.8	-0.6	-0.7	1.7	-0.2	-1.2	2.3	0.3	-0.5	0.7	47.3	1.39
116.4	29.1	1.80	14.4	2.35	62.7	67.8	115.3	-0.5	-0.7	1.6	-0.4	-0.8	2.2	0.1	-0.2	0.6	41.5	1.28
135.6	30.0	1.72	14.0	2.32	63.5	68.4	117.6	-0.5	-0.6	1.5	-0.4	-0.8	2.2	0.1	-0.2	0.6	36.4	1.20
154.8	27.1	1.65	13.7	2.43	64.1	66.4	110.5	-0.4	-0.6	1.5	-0.3	-0.9	2.2	0.1	-0.3	0.7	31.3	1.13
193.2	31.0	1.53	13.1	2.28	65.0	69.1	120.5	-0.4	-0.5	1.4	-0.4	-0.7	2.1	0.0	-0.2	0.7	26.9	1.02
250.8	29.8	1.41	12.5	2.33	66.1	68.3	117.1	-0.4	-0.4	1.3	-0.4	-0.8	2.2	0.0	-0.3	0.9	21.2	0.90
346.8	29.8	1.27	11.7	2.33	67.4	68.3	117.1	-0.3	-0.4	1.2	-0.4	-0.8	2.2	-0.1	-0.4	1.0	16.8	0.76
366.0	28.4	1.24	11.6	2.38	67.7	67.3	113.5	-0.3	-0.4	1.1	-0.4	-0.8	2.2	-0.1	-0.5	1.0	16.8	0.74
462.0	27.1	1.15	11.1	2.43	68.5	66.4	110.5	-0.3	-0.3	1.1	-0.3	-0.9	2.2	-0.1	-0.6	1.2	15.8	0.66

Table 2: Cutoff time and emission angle at each frequency for different L shells (OTD2)

MagModl: 0.133 45.20 13.50 0.190 0.485-0.191 165.0 :source mag long; 4.5 :L

Freq	SCET	rm	anglrB	rvd	slat	vlat	vlon	xsd			xvd			xvs		a bsv	Rmin
39.6	23.5	2.44	28.5	2.56	42.6	63.9	103.6	-1.7	-0.5	1.7	-0.3	-1.1	2.3	1.5	-0.6	0.7	127.8	1.79
58.8	21.8	2.16	25.7	2.63	46.1	62.7	100.8	-1.4	-0.4	1.6	-0.2	-1.2	2.3	1.2	-0.8	0.8	112.9	1.61
78.0	26.6	1.98	23.9	2.45	48.4	66.0	109.5	-1.3	-0.3	1.5	-0.3	-0.9	2.2	0.9	-0.6	0.8	106.3	1.44
97.2	28.1	1.85	22.7	2.39	50.1	67.1	112.8	-1.1	-0.3	1.4	-0.4	-0.9	2.2	0.8	-0.5	0.8	98.9	1.31
116.4	32.7	1.75	21.8	2.22	51.4	70.2	125.8	-1.1	-0.3	1.4	-0.4	-0.6	2.1	0.6	-0.3	0.7	95.0	1.21
135.6	34.1	1.67	21.0	2.17	52.5	71.0	130.8	-1.0	-0.3	1.3	-0.5	-0.5	2.1	0.5	-0.3	0.7	89.5	1.13
154.8	34.8	1.60	20.4	2.14	53.4	71.4	133.5	-0.9	-0.2	1.3	-0.5	-0.5	2.0	0.5	-0.2	0.7	84.1	1.06
193.2	35.5	1.49	19.4	2.11	54.8	71.6	136.2	-0.8	-0.2	1.2	-0.5	-0.5	2.0	0.4	-0.2	0.8	75.2	0.95
250.8	36.2	1.38	18.4	2.09	56.4	72.0	139.2	-0.7	-0.2	1.1	-0.5	-0.4	2.0	0.2	-0.2	0.8	65.4	0.83
346.8	38.8	1.24	17.1	2.00	58.3	72.8	151.7	-0.6	-0.2	1.1	-0.5	-0.3	1.9	0.1	-0.1	0.9	54.6	0.70
366.0	39.6	1.22	17.0	1.97	58.6	73.0	155.9	-0.6	-0.2	1.0	-0.5	-0.2	1.9	0.1	-0.1	0.8	53.0	0.68
462.0	38.4	1.13	16.2	2.01	59.9	72.7	149.6	-0.5	-0.1	1.0	-0.5	-0.3	1.9	0.0	-0.2	0.9	46.6	0.60

MagModl: 0.133 45.20 13.50 0.190 0.485-0.191 160.0 :source mag long; 5.0 :L

Freq	SCET	rm	anglrB	rvd	slat	vlat	vlon	xsd			xvd			xvs		a bsv	Rmin
39.6	23.5	2.46	26.2	2.56	45.4	63.9	103.6	-1.6	-0.6	1.8	-0.3	-1.1	2.3	1.4	-0.5	0.5	123.8	1.83
58.8	21.8	2.18	23.7	2.63	48.7	62.7	100.8	-1.4	-0.5	1.6	-0.2	-1.2	2.3	1.1	-0.7	0.7	107.6	1.63
78.0	26.6	2.00	22.2	2.45	50.8	66.0	109.5	-1.2	-0.4	1.5	-0.3	-0.9	2.2	0.9	-0.5	0.7	100.9	1.45
97.2	28.1	1.87	21.1	2.39	52.3	67.1	112.8	-1.1	-0.4	1.5	-0.4	-0.9	2.2	0.7	-0.5	0.7	93.0	1.32
116.4	32.7	1.76	20.3	2.22	53.6	70.2	125.8	-1.0	-0.4	1.4	-0.4	-0.6	2.1	0.5	-0.3	0.7	89.2	1.21
135.6	34.1	1.68	19.6	2.17	54.6	71.0	130.8	-0.9	-0.3	1.4	-0.5	-0.5	2.1	0.5	-0.2	0.7	83.4	1.13
154.8	34.8	1.61	19.0	2.14	55.4	71.4	133.5	-0.9	-0.3	1.3	-0.5	-0.5	2.0	0.4	-0.2	0.7	77.8	1.06
193.2	35.5	1.50	18.1	2.11	56.8	71.6	136.2	-0.8	-0.3	1.3	-0.5	-0.5	2.0	0.3	-0.2	0.7	68.7	0.95
250.8	36.2	1.38	17.2	2.09	58.3	72.0	139.2	-0.7	-0.2	1.2	-0.5	-0.4	2.0	0.2	-0.2	0.8	58.9	0.84
346.8	38.8	1.25	16.1	2.00	60.0	72.8	151.7	-0.6	-0.2	1.1	-0.5	-0.3	1.9	0.1	-0.1	0.8	48.9	0.70
366.0	39.6	1.23	15.9	1.97	60.3	73.0	155.9	-0.6	-0.2	1.1	-0.5	-0.2	1.9	0.0	0.0	0.8	47.7	0.68
462.0	38.4	1.14	15.2	2.01	61.5	72.7	149.6	-0.5	-0.2	1.0	-0.5	-0.3	1.9	0.0	-0.1	0.9	41.3	0.60

MagModl: 0.133 45.20 13.50 0.190 0.485-0.191 150.0 :source mag long; 6.0 :L

Freq	SCET	rm	anglrB	rvd	slat	vlat	vlon	xsd			xvd			xvs		a bsv	Rmin
39.6	23.5	2.50	22.9	2.56	49.8	63.9	103.6	-1.4	-0.8	1.9	-0.3	-1.1	2.3	1.1	-0.3	0.4	117.4	1.91
58.8	21.8	2.21	20.9	2.63	52.6	62.7	100.8	-1.2	-0.7	1.8	-0.2	-1.2	2.3	0.9	-0.5	0.6	97.8	1.65
78.0	26.6	2.02	19.6	2.45	54.5	66.0	109.5	-1.0	-0.6	1.6	-0.3	-0.9	2.2	0.7	-0.3	0.6	90.4	1.47
97.2	28.1	1.89	18.7	2.39	55.9	67.1	112.8	-0.9	-0.5	1.6	-0.4	-0.9	2.2	0.6	-0.3	0.6	81.4	1.33
116.4	32.7	1.78	18.0	2.22	57.0	70.2	125.8	-0.8	-0.5	1.5	-0.4	-0.6	2.1	0.4	-0.1	0.6	77.7	1.23
135.6	34.1	1.70	17.4	2.17	57.9	71.0	130.8	-0.8	-0.5	1.4	-0.5	-0.5	2.1	0.3	-0.1	0.6	71.6	1.15
154.8	34.8	1.63	17.0	2.14	58.6	71.4	133.5	-0.7	-0.4	1.4	-0.5	-0.5	2.0	0.3	-0.1	0.6	65.8	1.08
193.2	35.5	1.51	16.2	2.11	59.8	71.6	136.2	-0.7	-0.4	1.3	-0.5	-0.5	2.0	0.2	-0.1	0.7	56.6	0.97
250.8	36.2	1.39	15.4	2.09	61.2	72.0	139.2	-0.6	-0.3	1.2	-0.5	-0.4	2.0	0.1	-0.1	0.8	47.5	0.85
346.8	38.8	1.25	14.4	2.00	62.8	72.8	151.7	-0.5	-0.3	1.1	-0.5	-0.3	1.9	0.0	0.0	0.8	40.4	0.72
366.0	39.6	1.23	14.3	1.97	63.1	73.0	155.9	-0.5	-0.3	1.1	-0.5	-0.2	1.9	0.0	0.0	0.8	40.2	0.70
462.0	38.4	1.14	13.6	2.01	64.1	72.7	149.6	-0.4	-0.2	1.0	-0.5	-0.3	1.9	-0.1	-0.1	0.9	33.2	0.61

MagModl: 0.133 45.20 13.50 0.190 0.485-0.191 135.0 :source mag long; 7.0 :L

Freq	SCET	rm	anglrB	rvd	slat	vlat	vlon	xsd			xvd			xvs		a bsv	Rmin
39.6	23.5	2.52	20.6	2.56	53.1	63.9	103.6	-1.1	-1.1	2.0	-0.3	-1.1	2.3	0.8	0.0	0.3	111.5	1.97
58.8	21.8	2.23	18.9	2.63	55.7	62.7	100.8	-0.9	-0.9	1.8	-0.2	-1.2	2.3	0.7	-0.3	0.5	84.1	1.68
78.0	26.6	2.04	17.8	2.45	57.4	66.0	109.5	-0.8	-0.8	1.7	-0.3	-0.9	2.2	0.4	-0.2	0.5	75.5	1.49
97.2	28.1	1.90	17.0	2.39	58.6	67.1	112.8	-0.7	-0.7	1.6	-0.4	-0.9	2.2	0.3	-0.2	0.6	65.1	1.36
116.4	32.7	1.79	16.3	2.22	59.6	70.2	125.8	-0.6	-0.6	1.5	-0.4	-0.6	2.1	0.2	0.0	0.5	64.1	1.25
135.6	34.1	1.71	15.8	2.17	60.4	71.0	130.8	-0.6	-0.6	1.5	-0.5	-0.5	2.1	0.1	0.1	0.6	59.2	1.17
154.8	34.8	1.63	15.4	2.14	61.1	71.4	133.5	-0.6	-0.6	1.4	-0.5	-0.5	2.0	0.1	0.1	0.6	54.3	1.10
193.2	35.5	1.52	14.8	2.11	62.2	71.6	136.2	-0.5	-0.5	1.3	-0.5	-0.5	2.0	0.0	0.0	0.7	46.4	0.99
250.8	36.2	1.40	14.0	2.09	63.4	72.0	139.2	-0.4	-0.4	1.3	-0.5	-0.4	2.0	0.0	0.0	0.7	39.2	0.87
346.8	38.8	1.26	13.2	2.00	64.9	72.8	151.7	-0.4	-0.4	1.1	-0.5	-0.3	1.9	-0.1	0.1	0.8	37.8	0.74
366.0	39.6	1.24	13.0	1.97	65.1	73.0	155.9	-0.4	-0.4	1.1	-0.5	-0.2	1.9	-0.2	0.1	0.8	39.1	0.72
462.0	38.4	1.15	12.5	2.01	66.1	72.7	149.6	-0.3	-0.3	1.0	-0.5	-0.3	1.9	-0.2	0.0	0.9	30.4	0.63

MagModl: 0.133 45.20 13.50 0.190 0.485-0.191 130.0 :source mag long; 8.0 :L

Freq	SCET	rm	anglrB	rvd	slat	vlat	vlon	xsd			xvd			xvs		a bsv	Rmin
39.6	23.5	2.54	18.8	2.56	55.7	63.9	103.6	-0.9	-1.1	2.1	-0.3	-1.1	2.3	0.7	0.0	0.2	108.4	2.00
58.8	21.8	2.24	17.3	2.63	58.0	62.7	100.8	-0.8	-0.9	1.9	-0.2	-1.2	2.3	0.5	-0.3	0.4	75.8	1.71
78.0	26.6	2.05	16.3	2.45	59.6	66.0	109.5	-0.7	-0.8	1.8	-0.3	-0.9	2.2	0.3	-0.1	0.5	65.7	1.51
97.2	28.1	1.91	15.6	2.39	60.8	67.1	112.8	-0.6	-0.7	1.7	-0.4	-0.9	2.2	0.2	-0.1	0.5	54.6	1.38
116.4	32.7	1.80	15.1	2.22	61.7	70.2	125.8	-0.5	-0.7	1.6	-0.4	-0.6	2.1	0.1	0.0	0.5	55.2	1.27
135.6	34.1	1.71	14.6	2.17	62.4	71.0	130.8	-0.5	-0.6	1.5	-0.5	-0.5	2.1	0.0	0.1	0.5	51.5	1.19
154.8	34.8	1.64	14.3	2.14	63.1	71.4	133.5	-0.5	-0.6	1.5	-0.5	-0.5	2.0	0.0	0.1	0.6	47.4	1.12
193.2	35.5	1.53	13.7	2.11	64.1	71.6	136.2	-0.4	-0.5	1.4	-0.5	-0.5	2.0	-0.1	0.1	0.6	40.5	1.01
250.8	36.2	1.40	13.0	2.09	65.2	72.0	139.2	-0.4	-0.5	1.3	-0.5	-0.4	2.0	-0.1	0.0	0.7	34.6	0.89
346.8	38.8	1.26	12.2	2.00	66.6	72.8	151.7	-0.3	-0.4	1.2	-0.5	-0.3	1.9	-0.2	0.1	0.8	35.5	0.75
366.0	39.6	1.24	12.1	1.97	66.8	73.0	155.9	-0.3	-0.4	1.1	-0.5	-0.2	1.9	-0.2	0.1	0.7	37.3	0.73
462.0	38.4	1.15	11.6	2.01	67.7	72.7	149.6	-0.3	-0.3	1.1	-0.5	-0.3	1.9	-0.2	0.0	0.9	28.4	0.65

MagModl: 0.133 45.20 13.50 0.190 0.485-0.191 128.0 :source mag long; 8.6 :L

Freq	SCET	rm	anglrB	rvd	slat	vlat	vlon	xsd			xvd			xvs		a bsv	Rmin
39.6	23.5	2.55	18.0	2.56	57.0	63.9	103.6	-0.9	-1.1	2.1	-0.3	-1.1	2.3	0.6	0.0	0.2	107.0	2.01
58.8	21.8	2.25	16.6	2.63	59.3	62.7	100.8	-0.7	-0.9	1.9	-0.2	-1.2	2.3	0.5	-0.3	0.4	71.6	1.72
78.0	26.6	2.05	15.6	2.45	60.8	66.0	109.5	-0.6	-0.8	1.8	-0.3	-0.9	2.2	0.3	-0.1	0.4	60.4	1.52
97.2	28.1	1.91	15.0	2.39	61.9	67.1	112.8	-0.6	-0.7	1.7	-0.4	-0.9	2.2	0.2	-0.1	0.5	49.1	1.39
116.4	32.7	1.80	14.4	2.22	62.7	70.2	125.8	-0.5	-0.7	1.6	-0.4	-0.6	2.1	0.1	0.0	0.5	50.5	1.28
135.6	34.1	1.72	14.0	2.17	63.5	71.0	130.8	-0.5	-0.6	1.5	-0.5	-0.5	2.1	0.0	0.1	0.5	47.5	1.20
154.8	34.8	1.65	13.7	2.14	64.1	71.4	133.5	-0.4	-0.6	1.5	-0.5	-0.5	2.0	0.0	0.1	0.6	43.9	1.13
193.2	35.5	1.53	13.1	2.11	65.0	71.6	136.2	-0.4	-0.5	1.4	-0.5	-0.5	2.0	-0.1	0.0	0.6	37.7	1.02
250.8	36.2	1.41	12.5	2.09	66.1	72.0	139.2	-0.4	-0.4	1.3	-0.5	-0.4	2.0	-0.1	0.0	0.7	32.4	0.90
346.8	38.8	1.27	11.7	2.00	67.4	72.8	151.7	-0.3	-0.4	1.2	-0.5	-0.3	1.9	-0.2	0.1	0.7	34.4	0.76
366.0	39.6	1.24	11.6	1.97	67.7	73.0	155.9	-0.3	-0.4	1.1	-0.5	-0.2	1.9	-0.2	0.1	0.7	36.4	0.74
462.0	38.4	1.15	11.1	2.01	68.5	72.7	149.6	-0.3	-0.3	1.1	-0.5	-0.3	1.9	-0.3	0.0	0.8	27.4	0.66

REPORT DOCUMENTATION PAGE

Form Approved
OMB No. 0704-0188

1. AGENCY USE ONLY (Leave blank)	2. REPORT DATE	3. REPORT TYPE AND DATES COVERED
	July 9, 1993	Final June 4, 1992-July 9, 1993

4. TITLE AND SUBTITLE
Neptune High Latitude Emission:
Dependence of Angle on Frequency

5. FUNDING NUMBERS
NASW 4700

6. AUTHOR(S)
Constance Sawyer

7. PERFORMING ORGANIZATION NAME(S) AND ADDRESS(ES)
Radiophysics, Inc.
5475 Western Avenue
Boulder, CO 80301

8. PERFORMING ORGANIZATION REPORT NUMBER

9. SPONSORING/MONITORING AGENCY NAME(S) AND ADDRESS(ES)
NASA Headquarters
Washington, DC 20546

10. SPONSORING/MONITORING AGENCY REPORT NUMBER

11. SUPPLEMENTARY NOTES

12a. DISTRIBUTION/AVAILABILITY STATEMENT

12b. DISTRIBUTION CODE

13. ABSTRACT (Maximum 200 words)

Smooth broadband radio emission reached a maximum and then cut off as Voyager approached the north magnetic pole of Neptune. The time of each event depends on frequency, yielding information on radio source location and emission angle. In a preliminary analysis L-shell and magnetic longitude define radio- source locations in a dipole field. The emission angle at each frequency is identified with the angle between the magnetic-field direction at the source and the line of sight to Voyager 2 at the time of emission maximum. At each value of L in the range $6 < L < 9$, there is one source longitude for which emission angle varies smoothly from $\geq 90°$ at 40 kHz to as low as 20° at 462 kHz. A more complex magnetic-field model can give a qualitatively different result.

14. SUBJECT TERMS	15. NUMBER OF PAGES
Frequency-dependent radio emission angle magnetic L shell, occultation	10
	16. PRICE CODE

17. SECURITY CLASSIFICATION OF REPORT	18. SECURITY CLASSIFICATION OF THIS PAGE	19. SECURITY CLASSIFICATION OF ABSTRACT	20. LIMITATION OF ABSTRACT
Unclassified	Unclassified	Unclassified	Unlimited